

# SUB-MICROMETER RESOLUTION TRANSVERSE ELECTRON BEAM SIZE MEASUREMENT SYSTEM BASED ON OPTICAL TRANSITION RADIATION

A. Aryshev\*, N. Terunuma, and J. Urakawa, KEK, 1-1 Oho, Tsukuba, Ibaraki 305-0801, Japan  
S. T. Boogert, P. Karataev, JAI, RHUL, Egham, Surrey, TW20 0EX, UK.  
D. Howell, JAI, Oxford, Keble Road, Oxford OX1 3RH UK.

## Abstract

Optical Transition Radiation (OTR) appears when a charged particle crosses a boundary between two media with different dielectric properties has widely been used as a tool for transverse profile measurements of charged particle beams in numerous facilities worldwide. The resolution of the conventional monitors is defined by the Point Spread Function (PSF) dimension - the source distribution generated by a single electron and projected by an optical system onto a screen. For small electron beam dimensions, the PSF form significantly depends on various parameters of the optical system like diffraction of the OTR tails, spherical and chromatic aberrations, etc. In our experiment we managed to create a system which can practically measure the PSF distribution and using a new self-calibration method we are able to calculate transverse electron beam size. Here we represent the development, data analysis and novel calibration technique of a sub-micrometer electron beam profile monitor based on the measurements of the PSF shape, which visibility is sensitive to sub-micrometer electron beam dimensions.

## INTRODUCTION

In our recent reports [1, 2] we have demonstrated the status of the project on development of a sub-micrometer resolution transverse electron beam size measurement system based on optical transition radiation. Recent results have clearly demonstrated that the method based on the analysis of the OTR PSF structure [3] visibility gives an opportunity to measure the beam size with a sub-micrometer resolution. In this report we shall represent the current status of the project focusing on detailed explanation of the data analysis and self calibration procedure. The brief explanation on error propagation and final resolution calculus will be given.

The experiment was performed at ATF-II extraction line [4] and experimental setup including description of the accelerator, vacuum manipulator, OTR target, timing system, DAQ system as well as the laser alignment system will be excluded since it was well described in [1].

## DATA ANALYSIS AND DISCUSSION

CCDs are silicon semiconductor devices which use a reverse-biased p-n junction (essentially a photodiode) to absorb photons and produce charges representing sensed

\*alar@post.kek.jp

pixels. The accumulated electrons in each pixel get represented by a number in “units” of a DN (Data Number) or ADU (Analogue-to-Digital Unit). Inverse-Gain is this conversion factor in dimensionless units of e-/DN. Noise in photon counting is referred to as “Poisson” noise associated with counting statistics (appropriate to counting the number of photons that arrive each time interval). For the Poisson distribution and taking into account Inverse-Gain, the standard deviation is  $STD_{pixel} = \sqrt{gain \cdot N}$ , where  $N$  is the number of detected events [5]. It is important to start from this error calculation. The next step in image processing is pixel-by-pixel background subtraction with correct error propagation:

$$STD_{pixel}^{sub} = \sqrt{STD_{pixel}^{image^2} + STD_{pixel}^{background^2}}$$

To deduct image noise and remove bad pixels the median window filter was used. The basic idea was to iterate a 3x3 pixel subframe through the image, replacing central pixel with the neighbouring median if it runs over a given threshold [6].

After that, a portion of resulting image to produce horizontal or vertical projections summing rows or columns respectfully was extracted and pixel scale of the projection was converted into microns as follows:

$$X_i^{um} = \frac{X_i^{pixel} \cdot binning \cdot pixel\ size}{magnification\ factor}$$

The magnification factor for the data set under analysis was  $10.69 \pm 0.08 \mu m$  [2].

To analyze the vertical projection, especially OTR spot minimum behavior, a special empirically found fit function had been introduced [1]:

$$f(x) = a + \frac{b}{1 + [c(x - \Delta x)]^4} \left[ 1 - e^{-2c^2 \sigma^2} \cos[c(x - \Delta x)] \right] \quad (1)$$

Numerical fit which uses the Levenberg-Marquardt method to calculate the best fit parameters that minimize the weighted mean squared error between the observations in data amplitude and the best nonlinear fit was used and the errors of each point of the resulting fit curve was calculated as:

$$\Delta f(x) = \sqrt{\sum (f(x))_i^2 \cdot \Delta_i^2} \quad (2)$$

, where  $(f(x))_i^2$  are squares of partial derivatives of (1) with respect to all free fitting parameters (a,b,c,d,σ)

and  $\Delta_i^2$  are squares of fitting parameters standard deviations.

Horizontal projection was processed in the same manner employing symmetric Gaussian fit which directly gives horizontal RMS beam size of  $15.33 \pm 0.4 \mu\text{m}$  (for a current shot). Resulting plots are shown at Figure 1.

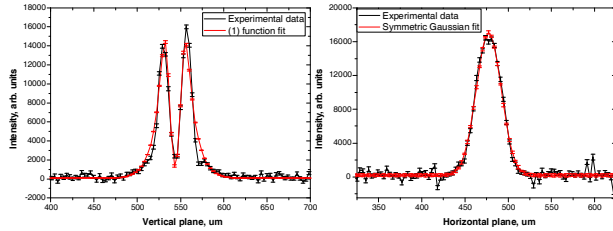


Figure 1: Two CCD image projections: horizontal (right) and vertical (left).

From this point we will be focused on analysis of a vertical projection only, since Gaussian fit of the horizontal projection does not required any calibration and returns an absolute measured value.

It is important to mention that to perform a self calibration, one has to have a data set which contains a variation of the vertical beam size, and for example quadrupole scan. This scan should be taken after careful beamline tuning including beam based alignment, so change in a quadrupole field does not change transverse electron beam position. Otherwise one will have to increase image projection window width, or introduce variation in shot-by-shot integration window position what could lead to degradation of a resolution.

Before starting self-calibration it is important to find a value of a local minimum (at the centre of the curve, between lobes), and the value of a local maximum with corresponded errors for every file in whole dataset  $I_{\min}, I_{\max}, \Delta I_{\min}, \Delta I_{\max}$ , and then calculate its ratio  $I_{\min} / I_{\max}$  as well as its error:

$$\Delta_{I_{\min} / I_{\max}} = \sqrt{\sum (I_{\min} / I_{\max})_i^2 \cdot \Delta I_i^2} = \sqrt{\frac{\Delta I_{\min}^2}{I_{\max}^2} + \frac{I_{\min}^2 \cdot \Delta I_{\max}^2}{I_{\max}^4}}$$

, then find the file with smallest  $I_{\min} / I_{\max}$ . This file should be used for calibration.

After that, re-generate fit curve  $f(x)$  with errors  $\Delta f(x)$  for the calibration file substituting zeros for horizontal and vertical offsets (a,c) and  $\sigma$ . Convolute it with Gaussian as follows:

$$F_j^{Convolution} = \frac{\sum_{i=1}^N f_i(x_i) \cdot \exp\left(\frac{-(x-x_i)^2}{2\sigma_{conv}^2}\right)}{\sum_{i=1}^N \exp\left(\frac{-(x-x_i)^2}{2\sigma_{conv}^2}\right)} \quad (3)$$

Propagate errors  $\Delta f(x)$  through convolution according to (2), repeat convolution  $N$  times varying  $\sigma_{conv}$  from 0 to  $M$  with a fine step. For each iteration, find  $I_{\min} / I_{\max}$  and calculate its errors  $\Delta_{I_{\min} / I_{\max}}$  resulting in calibration curve. Further, one needs to fit calibration curve  $\sigma_{conv} = f(I_{\min} / I_{\max})$ , where errors  $\Delta_{I_{\min} / I_{\max}}$  appears as horizontal errors. To a good approximation, the uncertainty in y, because of the errors in x, is the error in x times the slope of the line where slope of the line is  $\Delta y_i / \Delta x_i$ .

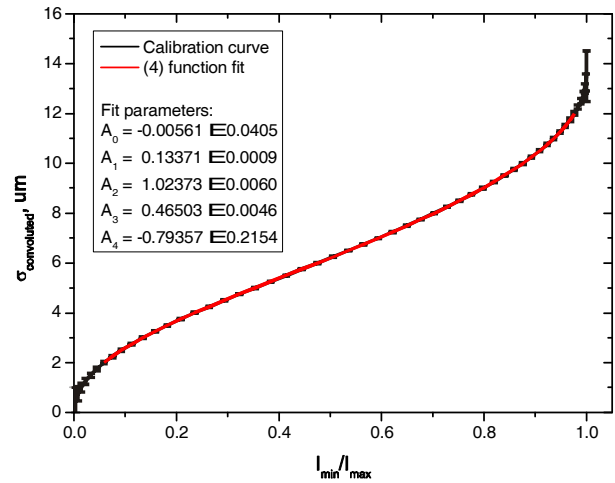


Figure 2: Calibration function along with the fit (4).

To fit resulting calibration curve another empirical function was introduced:

$$y = A_0 + \frac{1}{A_1} \cdot \left( -\ln\left(1 - \frac{x}{A_2}\right) \right)^{A_3} + A_4 \cdot x^{12} \quad (4)$$

Again, to propagate errors we used (2), where  $(f(x))_i^2$  are squares of partial derivatives of (4) with respect to all fitting parameters ( $A_0, A_1, A_2, A_3, A_4, x$ ) and  $\Delta_i^2$  are squares of fitting parameters STD-es and  $x$  in this case is  $I_{\min} / I_{\max}$  with corresponding error  $\Delta_{I_{\min} / I_{\max}}$ . Figure 2 represents resulting calibration function along with the fit (4).

At this point it is possible to analyze all files in a data set, extracting  $I_{\min} / I_{\max}$  and  $\Delta_{I_{\min} / I_{\max}}$  for each file and convert it to real vertical RMS beam sizes using calibration fit parameters and its standard deviations.

As we mention before, it is important to use the file with smallest  $I_{\min} / I_{\max}$  for calibration. Figure 4 (left) demonstrates Q-scan minimum RMS vertical beam size variation versus a few different calibration files. Labels

represents QD18X strengths for each calibration file according to Figure 3 (right).

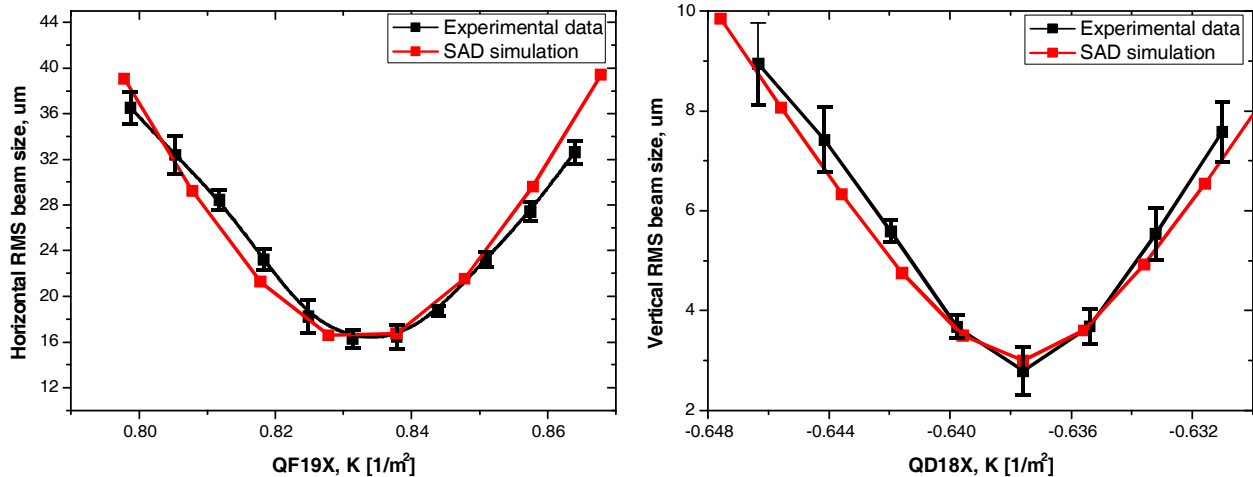


Figure 3: Horizontal RMS beam size as a function of the QF19X strength (left) and Vertical RMS beam size as a function QD18X strength (right). SAD predictions of the vertical and horizontal beam sizes are also shown.

Another important parameter in OTR image processing is the image projection window width. Its effect on calculated Q-scan minimum RMS vertical beam size is represented on Figure 4 (right).

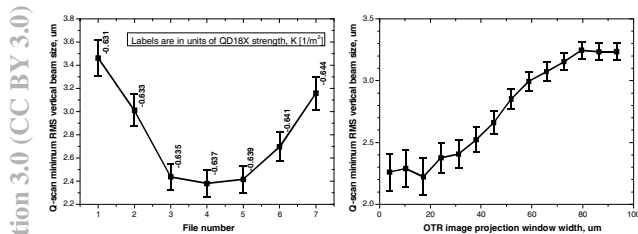


Figure 4: Q-scan minimum RMS vertical beam size variation versus a few different calibration files (left), and versus image projection size window width versus (right).

## CONCLUSION

In this paper we present the experimental results which clearly demonstrate that the method based on the analysis of the PSF structure visibility gives an opportunity to measure the beam size with a sub-micrometer resolution. In order to improve the beam size measurement technique additional efforts toward the optimization of the optical system, and better understanding of the beam size effect has been taken.

To be able to achieve our goals and demonstrate better resolution achromat lens (to minimize the chromatic aberrations in the optical system) was employed. Also a few more optical filters covering the wavelength range from 350 to 800nm with 50nm step was used to investigate the spectral characteristics of the OTR PSF in details. The results will be represented in a successive paper.

## ACKNOWLEDGEMENTS

We would like to thank the ATF extraction line Laser-Wire collaboration for giving us an opportunity to conduct the experiment. This research was partially supported by DAIWA Anglo-Japanese Foundation, LC-ABD collaboration, partial support from the “Grant-in-Aid for Creative Scientific Research of JSPS (KAKENHI 17GS0210)” project, European Commission under the FP7 Research Infrastructures project EuCARD, grant agreement no.227579, and Quantum Beam Technology Program of the Ministry of Education, Science, Sports, Culture and Technology of Japan (MEXT).

## REFERENCES

- [1] A.Aryshev, et. al., Journal of Physics: Conference Series 236 (2010) 012008.
- [2] A. Aryshev, et. al., IPAC’10, June 2008, Kyoto, Japan, MOPEA053
- [3] P.Karataev, et al., The First Observation of the Point Spread Function of Optical Transition Radiation, submitted to Physical Review Letters, October 2009.
- [4] P. Bambade et al. (ATF Collaboration), PRST-AB 13, 042801 (2010).
- [5] S. B. Howell, Handbook of CCD astronomy, Cambridge University Press, 2000.
- [6] A. Bovik, The essential guide to image processing, Elsevier, 2009.